Cell, Vol. 75, 899–912, December 3, 1993, Copyright © 1993 by Cell Press

High Levels of c-*rel* Expression Are Associated with Programmed Cell Death in the Developing Avian Embryo and in Bone Marrow Cells In Vitro

Corinne Abbadie,*† Nell Kabrun,‡ F. Bouali,* Jana Smardova,‡ Dominique Stéhelin,* Bernard Vandenbunder,* and Paula J. Enrietto‡
*Laboratoire d'Oncologie Moleculaire
Centre National de la Recherche Scientifique
Unité de Récherche Associée 1160
Institut Pasteur
1 rue Calmette
59019 Lille Cedex
France
†Laboratoire de Biologie du développement
Université Lille 1
59655 Villeneuve d'Ascq Cedex
France
‡Department of Microbiology
State University of New York at Stony Brook
Stony Brook, New York 11794

Summary

To determine the physiological processes in which the transcription factor c-Rel may act, we have examined its pattern of expression in the avian embryo by in situ hybridization. These studies showed that c-*rel* is expressed ubiquitously at low levels and at high levels in isolated cells undergoing programmed cell death by apoptosis or autophagocytosis. To further establish a functional link between expression of *c-rel* and cell death, we examined the biological consequences of *c-rel* overexpression in vitro. In primary avian fibroblasts, overexpression of *c-rel* leads to transformation and dramatic life span extension. In contrast, bone marrow cells expressing high levels of *c-rel* undergo a process of programmed cell death displaying features of both apoptosis and autophagocytic cell death. Thus, these experiments suggest a critical role for *c-rel* not only in the control of cell proliferation, but also in the induction of cell death.

Introduction

Central to our understanding of cellular growth control and differentiation is the identification of the genes involved in the regulation of these processes. It has become clear that oncogenes play key roles in the control of normal growth (Reddy et al., 1988). One such gene, c-*rel*, has been implicated in the regulation of normal hematopoiesis by virtue of its pattern of expression and the transforming properties of its viral homolog, v-*rel*. Northern blot analysis of embryonic and adult avian tissues showed that c-*rel* was expressed predominantly in hematopoietic organs such as the bursa of Fabricius, thymus, spleen, and bone marrow (Brownell et al., 1987; Moore and Bose, 1989; Grumont and Gerondakis, 1990a, 1990b). v-*rel* causes rapidly fatal leukemia in birds and in vitro transforms and extends the life span of avian hematopoietic cells and fibroblasts (Beug et al., 1981; Lewis et al., 1981; Morrison et al., 1991). Interestingly, v-*rel*-transformed bursal lymphocytes become resistant to apoptosis induced by radiation, dexamethasone, or calcium ionophore (Neiman et al., 1991). These data strongly suggest a role for the Rel proteins in the control of cell growth, cell death, or both.

The biochemical mechanism by which c-*rel* regulates cell growth can be inferred from its homology to a growing family of transcription factors. This family includes the NF-κB subunits p50 and p65 (Kieran et al., 1990; Nolan et al., 1991), *relB* (Ryseck et al., 1992), *lyt-10*, the product of a gene first identified in a chromosomal translocation associated with chronic lymphocytic leukemia (Neri et al., 1991), and the *Drosophila* morphogen *dorsal* (Steward et al., 1985). These genes share homology over an amino terminal region of about 300 amino acids, termed the Rel homology domain, and exhibit similar biochemical properties. C-Rel, like NF-κB, is part of a multiprotein complex (Simek and Rice, 1988; Morrison et al., 1989; Davis et al., 1990, 1991; Kochel et al., 1991; Nolan and Baltimore, 1992). Two members of this complex, IκB and p124 (the avian homolog of the mammalian p105 NF-κB precursor), are ankyrin repeat-containing proteins which may be involved in cytoplasmic sequestration and inhibition of DNA binding (Baeuerle, 1991; Kerr et al., 1991; Inoue et al., 1992; Capobianco et al., 1992; Rice et al., 1992). Both c-Rel and NF-κB bind consensus κB oligonucleotides and have been postulated to regulate transcription of a number of different genes (reviewed by Baeuerle, 1991; Hannink and Temin, 1990; Capobianco and Gilmore, 1991; Inoue et al., 1991; Ballard et al., 1992; Fujita et al., 1992; Hansen et al., 1992; Kochel and Rice, 1992; Nakayama et al., 1992; Tan et al., 1992; Perkins et al.,1992).

To understand the functional role of c-*rel* in normal cell growth and differentiation, we have taken two approaches. First, we examined the pattern of expression of c-*rel* in the developing embryo by in situ hybridization and show here that c-*rel* is expressed ubiquitously at low levels in the developing embryo. Surprisingly, high levels of expression are observed in cells undergoing two kinds of programmed cell death: apoptosis and autophagic degeneration. While these results suggest a role for c-*rel* in the process of cell death, they do not prove a functional link. Therefore, to demonstrate the direct involvement of c-*rel* in the process of programmed cell death, we analyzed the consequences of c-*rel* overexpression in vitro in two different cell types. Infection of avian fibroblasts with a c-*rel*-containing retrovirus leads to morphological transformation and, most remarkably, a dramatic extension of their life span in culture. In contrast, bone marrow cells overexpressing c-Rel undergo a process of programmed cell death which displays features of both apoptosis and autophagocytic degeneration. Thus, we propose that under certain conditions, the transcription factor encoded by c-*rel* may induce programmed cell death, perhaps by activating a set of death genes.

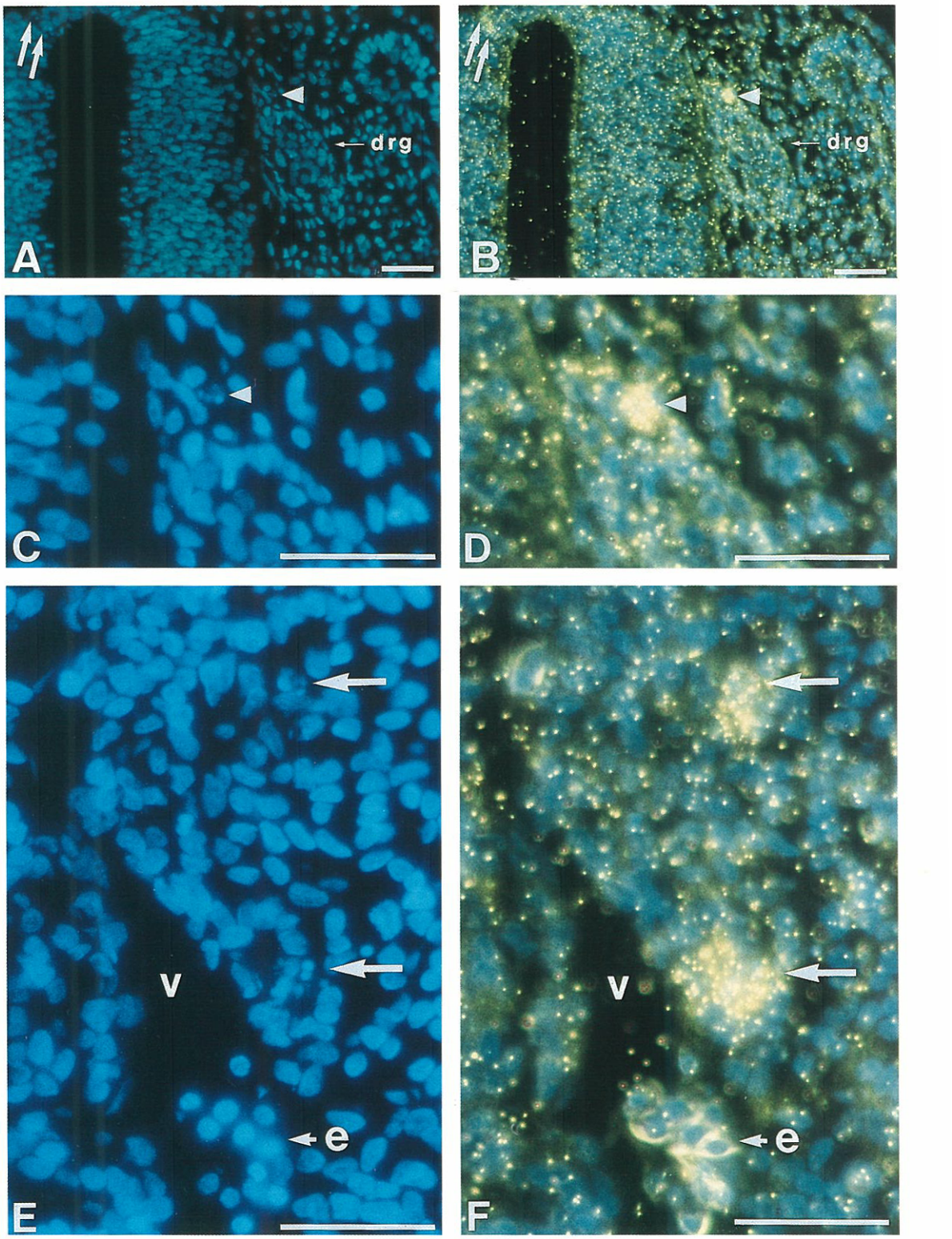

Figure 1. Examples of the Variety of Cellular Types Undergoing Apoptosis

Transverse sections through a chick embryo at E3 were hybridized with an antisense c-*rel* probe and stained with a DNA fluorescent dye. Sections were observed under ultraviolet illumination to determine the nuclear morphology (A, C, and E) and dark-field illumination to visualize silver grains (B, D, and F). Bars represent 40 μm.

(A and B) Cells within the spinal chord (arrows) and among migrating neural crest cells (arrowhead) colonizing the dorsal root ganglion (drg) exhibit high levels of c-*rel* expression.

Results

c-*rel* Is Highly Expressed in Cells Undergoing Programmed Cell Death

The pattern of expression of the protooncogene c-*rel* during avian development was studied by in situ hybridization using [^{35}S]RNA probes against full-length c-*rel* RNAs and a c-*rel* specific 2.8 kb probe (see Experimental Procedures for details). Under high stringency conditions, these two probes gave the same results, qualitatively and quantitatively. Therefore, we consider the patterns obtained either with the full-length or the 2.8 kb probe reflective of c-*rel* expression without any cross-reaction with other NF-κB family members.

c-*rel* expression was studied in chicken embryos from embryonic stage E3 to E9.5. The distribution and density of silver grains indicate that c-*rel* is expressed at low levels in most tissues at every stage of development studied. While the levels of expression were quite low, comparison with control sense probe hybridizations revealed that these low levels of expression were nonetheless significant. In contrast, a strong hybridization signal was observed in various parts of the embryo in some isolated cells that shared a common nuclear morphology. Staining with the intercalating dye Hoechst 33258 showed that the nuclei were fragmented into two or more pieces of variable size, each fragment having a round shape and containing highly condensed chromatin. In some cases, the nuclei were not fragmented, but the chromatin was condensed and localized close to the nuclear envelope. These two nuclear morphologies are typical of cells dying by apoptosis (Wyllie et al., 1980). At E3 and E4.5, apoptotic cells were found in a number of tissues including the epithelium of the third and fourth branchial furrows, the mesenchyme of the branchial arches, the chord, the central nervous system, the migrating neural crest (Figures 1A–1D), some nervous ganglia, the mesenchyme in the vicinity of some vessels (Figures 1E and 1F), the cephalic mesenchyme, the spleen primordia, and the gonad primordia. In all these tissue types, different as they are, the majority of apoptotic cells expressed c-*rel* at high levels.

Since the occurrence of apoptosis at these early stages of development is not well documented, we investigated the expression of c-*rel* in the limb bud for which programmed cell death has been described in great detail. In the limb bud, there are four major areas of cell death (Hinchliffe and Ede, 1973): the anterior and posterior necrotic zones, the opaque patch in the central limb mesenchyme, and the interdigital necrotic zones. On morphological grounds, Clarke (1990) distinguished three types of developmental cell death: type 1, which represents bona fide apoptosis since the destruction of the cell is achieved primarily by heterophagy; type 2, characterized by the presence of autophagic vacuoles; and type 3, which shares several common features with necrosis. We examined c-*rel* expression in these four areas of cell death from E5 to E9.5, in the hind limb as well as in the forelimb. We observed apoptotic cells labeled with the c-*rel* probe in the opaque patch, particularly at E5 (Figure 2A), in the anterior and posterior necrotic zones (data not shown), and in the interdigital mesenchyme (Figures 2D and 2F). In this last tissue, apoptotic bodies were a minority, scattered among numerous atypical cellular fragments, which contained noncondensed chromatin. These fragments may be autophagic cells (type 2), which by in situ hybridization clearly express higher levels of c-*rel* than does the surrounding healthy mesenchyme (Figure 2B).

The Presence of the c-Rel Protein in Chicken Tissues Is Confirmed by Western Blot

To demonstrate the presence of c-Rel protein in the tissues examined, Western blots were performed using extracts of total embryos at E3 and E4.5, brain, heart, liver, and intestine of E6 embryo and limb buds from E5.5 to E9.5. Blots were incubated with a purified antibody directed against the 15 amino acids at the carboxy terminus of the c-Rel protein (P. E., unpublished data). As can be seen (Figures 3A and 3B), in all tissues this serum reacts with a major band of 68 kd, the chicken c-Rel protein (Simek and Rice, 1988). The additional lower molecular weight proteins may represent nonspecific cross-reactive species. Clearly, c-Rel proteins are detected in tissues where programmed cell death occurs as well as in tissues where it does not, such as the liver at E6 (Figure 3A, lane 5). Therefore, proteins detected by Western blot analysis presumably included those of healthy and dying cells.

Cleavage of Nuclear Chromatin

In situ hybridization experiments described above revealed an intense hybridization signal over apoptotic cells in the young embryo and in the developing limb bud. However, the identification of apoptotic cells relied here only on morphological criteria. To confirm that apoptosis occurred in these tissues, we examined a biochemical marker for apoptosis: the cleavage of nuclear chromatin by an internucleosomal endonuclease. Such cleaved DNA is resolved as a ladder composed of 180 bp fragments and multiples thereof (Wyllie et al., 1980). DNA ladders have never been documented in chick embryos, presumably because apoptotic cells are scarce, as shown in Figures 1 and 2. Therefore, to increase the sensitivity of detection of chromatin cleavage, we radioactively end-labeled DNA preparations from embryos with Klenow polymerase (Rösl, 1992). As a positive control, we used S49.1 cells

(C and D) Higher magnification of the same section showing that the neural crest cell expressing high levels of c-*rel* has an apoptotic, fragmented nucleus.

(E and F) High magnification of an area in the vicinity of a vessel (v) where apoptotic cells expressing high levels of c-*rel* are often found. Erythrocytes (e) in the vessel lumen display nonspecific light scattering.

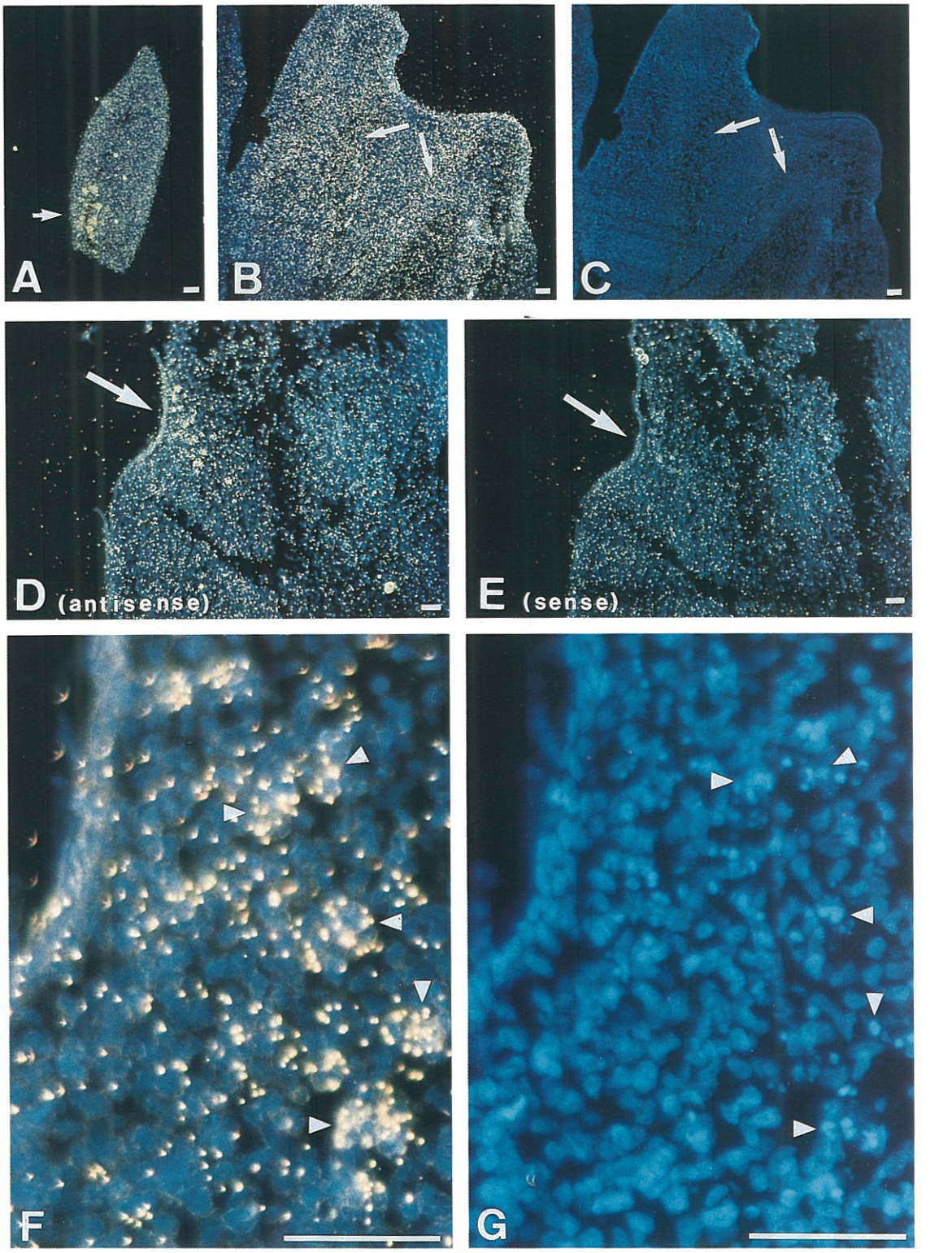

Figure 2. *c-rel* Expression in the Hindlimb

Limbs were sectioned longitudinally, hybridized with an antisense (A, B, D, and F) or a sense (E) *c-rel* probe, and stained with a DNA fluorescent dye. Sections were observed under ultraviolet illumination only (C and G) or under ultraviolet plus dark-field illumination (A, B, D, E, and F).

(A) The limb bud at E5 contains apoptotic cells expressing high levels of *c-rel* (see arrows) in the opaque patch at the opposite of the apex.

(B and C) In the limb bud at E7, *c-rel* is expressed less in the healthy mesenchyme than in the loose interdigital mesenchyme (arrows) that appears to degenerate by autophagic cell death.

(D) In other areas of the interdigital mesenchyme at E7, a few cells expressed *c-rel* at a high level.

(E) Serial section hybridized with a control sense probe.

(F and G) Higher magnification of section D shows that the cells expressing *c-rel* have the morphology of cells dying by apoptosis (arrowheads).

Bars represent 40 μM.

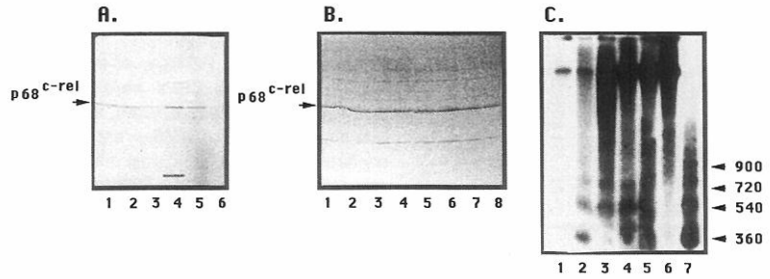

Figure 3. Western Blots of Embryonic Chicken Proteins Stained with an Anti-c-Rel Antibody and Characterization of DNA Ladders

(A) Western blot of proteins from total embryos at E3 (lane 1), E4.5 (lane 2), and brain (lane 3), heart (lane 4), liver (lane 5), and intestine (lane 6), all at E6.

(B) Western blot of proteins from the forelimb at E5.5, E7, E8, and E9.5 (lanes 1, 3, 5, and 7, respectively) and from the hindlimb at the same stages (lanes 2, 4, 6, and 8). The p68$^{c\text{-}rel}$ protein is indicated with a bold arrow. The additional lower and upper molecular weight proteins may represent cross-reactive species.

(C) ^{32}P-end-labeled total DNA from different tissues was analyzed on a 1.8% agarose gel. Total DNA from S49.1 cells, in which apoptosis was induced by 1 μM dexamethasone during 24 hr, was used as a control. The gel was loaded as follows: E3, 1 μg (Lane 1); E4.5, 1 μg (Lane 2); hindlimb at E5.5, E6, and E7, 0.75 μg (lanes 3, 4, and 5, respectively); liver at E7, 0.5 μg (Lane 6); and S49.1, 0.5 μg (Lane 7).

(Figure 3C, lane 7), a mouse lymphoma line which undergoes apoptosis in response to glucocorticoids (Ucker, 1987). As shown in Figure 3C, typical chromatin fragmentation can be observed in DNA extracted from total embryos at E4.5 (Fig 3C, lane 2) and from hindlimbs at E5.5, E6, and E7 (Figure 3C, lanes 3, 4, and 5, respectively). The weak intensity of bands reflects the small number of apoptotic cells observed on histological sections. At E3 (Figure 3C, lane 1), for example, no ladder is detected, probably because apoptotic cells are too scarce. In contrast, the liver at E7 is negative (Figure 3C, lane 6), consistent with the fact that apoptotic bodies were never observed in this tissue at that stage.

Biological Consequences of Overexpression of c-*rel* In Vitro

Having demonstrated high levels of c-*rel* in embryonic cells undergoing programmed cell death, we sought to establish a functional link between c-*rel* expression and cell death. Previous reports suggested that overexpression of avian c-*rel* in vitro failed to transform chicken embryo fibroblasts or spleen cells (Capobianco et al., 1990). However, these experiments were carried out using a replication-defective c-*rel* virus that required helper virus for propagation. We and others (Barth and Humphries, 1988; Morrison et al., 1989) showed previously that helper virus cytotoxicity has a profound effect on the biological activity of v-*rel*. Thus, in these studies, we used a replication-competent viral vector RCAS (Hughes et al., 1987) that was used previously to show transformation of avian fibroblasts and bone marrow cells in vitro by v-*rel* (Boehmelt et al., 1992; Morrison et al., 1989).

Construction and Expression of RCAS-c-*rel*

The avian c-*rel* cDNA, molecularly cloned from bursal and HP46 cDNA libraries (Kabrun et al., 1990), was placed in the viral vector RCAS (RCAS–c-*rel* in Figure 4A) and transfected into normal chicken embryo fibroblasts. After four passages, cells were tested for exogenous c-*rel* gene expression by Western blot with polyclonal antibody (SB66) that recognizes c-Rel and v-Rel (Morrison et al., 1989). High levels of p68$^{c\text{-}rel}$ were seen in RCAS–c-*rel*–transfected cells (Figure 4B) as compared with endogenous levels in control RCAS vector–transfected chicken embryo fibroblasts (CEFs) (Figure 4B). Positive control RCAS–v-*rel*–transfected fibroblasts were also examined (Morrison et al., 1989).

Subcellular Localization and Biochemical Properties of Overexpressed c-Rel in Chicken Embryo Fibroblasts

Before characterizing the biological consequences of c-*rel*

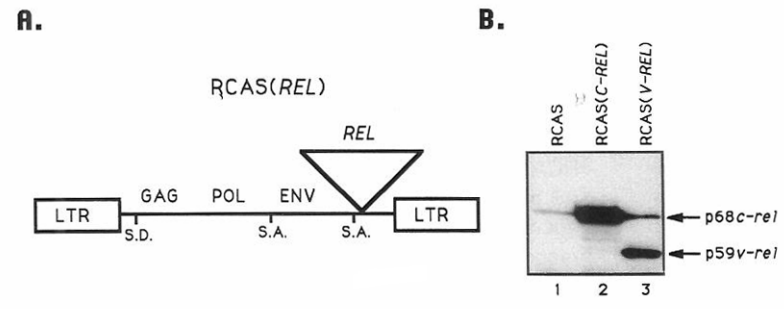

Figure 4. Schematic Representation of RCAS–c-*rel* or RCAS–v-*rel* Retroviral Expression Vector

(A) LTR, GAG, POL, and ENV represent regions of proviral DNA required for replication, gene expression, or both. *Rel* represents either exogenous c-*rel* or v-*rel* cDNA cloned into a ClaI site downstream of the envelope gene, where it is expressed from a subgenomic message; S. D. is splice donor and S. A. is splice acceptor.

(B) Expression of c-Rel or v-Rel protein in CEFs infected with RCAS, RCAS–c-*rel*, or RCAS–v-*rel* virus. Cells infected with RCAS (lane 1), RCAS–c-*rel* (lane 2), or RCAS–v-*rel* (lane 3) were lysed in sample buffer and subjected to Western blot analysis. Blots were probed with SB66, a polyclonal antibody that recognizes both c-Rel and v-Rel proteins. The positions of p68$^{c\text{-}rel}$ and p59$^{v\text{-}rel}$ are indicated.

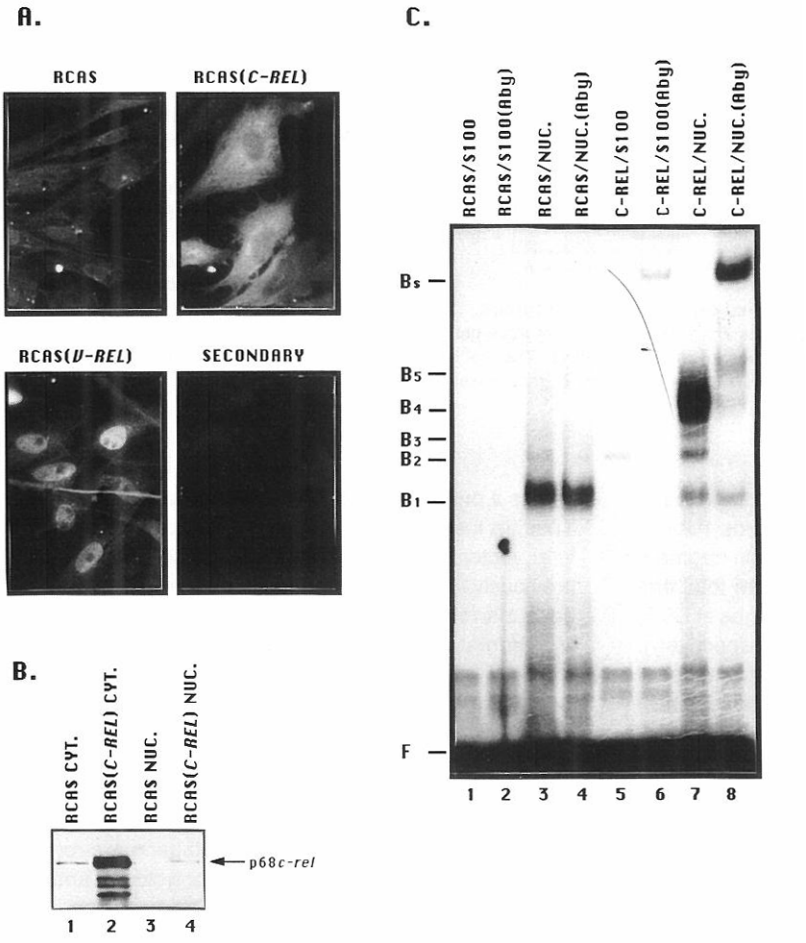

Figure 5. Biochemical Characterization of c-Rel and v-Rel

(A) RCAS-infected, RCAS–c-*rel*–infected, or RCAS–v-*rel*–infected CEFs were fixed with paraformaldehyde, permeabilized, and stained with anti-*rel* polyclonal SB66, = and a secondary fluorescein-conjugated goat anti-rabbit immunoglobulin. Alternatively, the secondary antibody was used alone as a control (labeled secondary).

(B) RCAS-infected or RCAS–c-*rel*–infected CEFs were biochemically separated into nuclear and cytoplasmic fractions. Fractions were subjected to Western blot analysis and probed with SB66 polyclonal antibody. Cytoplasmic fractions (lanes 1 and 2) or nuclear fractions (lanes 3 and 4) are indicated above the figure. The position of $p68^{c\text{-}rel}$ is indicated to the right of the figure.

(C) Electrophoretic mobility shift asays were done utilizing nuclear (lanes 3, 4, 7, and 8) and S100 (lanes 1, 2, 5, and 6) extracts from RCAS-infected (lanes 1–4) or RCAS–c-*rel*-infected (lanes 5–8) CEFs and a double-stranded oligonucleotide containing a κB-binding site sequence (Kabrun et al., 1991). Gel shift reactions were carried out in the presence (lanes 2, 4, 6, and 8) or absence (lanes 1, 3, 5, and 7) of antibody to *rel* (SB66). F and B_n represent free and bound κB probe, respectively. B_s represents a supershifted band with reduced mobility in the presence of antibody to c-Rel or v-Rel.

overexpression, it was critical to demonstrate that the protein was biochemically functional. Therefore, the localization and DNA binding properties of overexpressed c-Rel was analyzed in avian fibroblasts. Immunofluorescent staining of RCAS–c-*rel*-infected, RCAS–v-*rel*-infected, and control RCAS-infected cells was carried out as described in Experimental Procedures using the polyclonal antibody SB66 (Morrison et al., 1989). As can be seen in Figure 5A, and as previously reported, v-Rel is found at high levels in the nucleus of RCAS–v-*rel* CEFs (Gilmore and Temin, 1986; Morrison et al., 1992, 1989). While the majority of the overexpressed c-Rel protein localized in the cytoplasm, there appeared to be a significant quantity in the nucleus as well (see below). The marginal staining of control RCAS CEFs probably represents endogenous c-Rel since secondary antibody showed little background staining. To confirm these localization results, cytoplasmic and nuclear fractions (Morrison et al., 1992, 1989) from RCAS–c-*rel* CEFs were analyzed by Western blot. As can be seen in Figure 5B, endogenous c-Rel was present in the cytoplasm of RCAS CEFs; however, at the resolution of this assay, no detectable protein was observed in the nucleus. In sharp contrast, the nuclear fraction from RCAS–c-*rel* CEFs contained c-Rel protein at detectable levels, confirming the immunofluorescence results. As expected, high levels of c-Rel were found in the RCAS–c-*rel* cytoplasmic fraction. Lower molecular weight proteins observed probably represent proteolytic cleavage products of $p68^{c\text{-}rel}$.

As with NF-κB, cytoplasmic sequestration of inactive c-Rel is thought to occur via association with either of the inhibitor proteins IκB or p124, the avian equivalent of the NF-κB precursor p105 (Davis et al., 1991; Nolan and Baltimore, 1992; Rice et al., 1992). Since most of the c-Rel protein in RCAS–c-*rel* CEFs was sequestered in the cytoplasm, we wanted to determine if cytoplasmic c-Rel, nuclear c-Rel, or both were able to bind to a consensus κB site. Electrophoretic mobility shift assays were performed using S100 or nuclear extracts from RCAS or RCAS–c-*rel* CEFs and a radioactively labeled oligonucleotide containing the consensus κB-binding site (Dignam et al., 1983; Kabrun et al., 1991). While the S100 fraction from RCAS CEFs (Figure 5C, lane 1) contained no detectable κB binding activity, RCAS nuclear extracts exhibited an activity (Figure 5C, lane 3) unrelated to Rel as it was not recognized by the SB66 antiserum (Figure 5C, lane 4). At high protein concentrations, however, a nuclear species could be detected in normal cells that is reactive with the SB66 antibody (data not shown).

As can be seen in Figure 5C (lane 5), RCAS–c-*rel* S100 extract contained very little DNA binding activity, suggesting an inhibition of cytoplasmic c-Rel perhaps due to

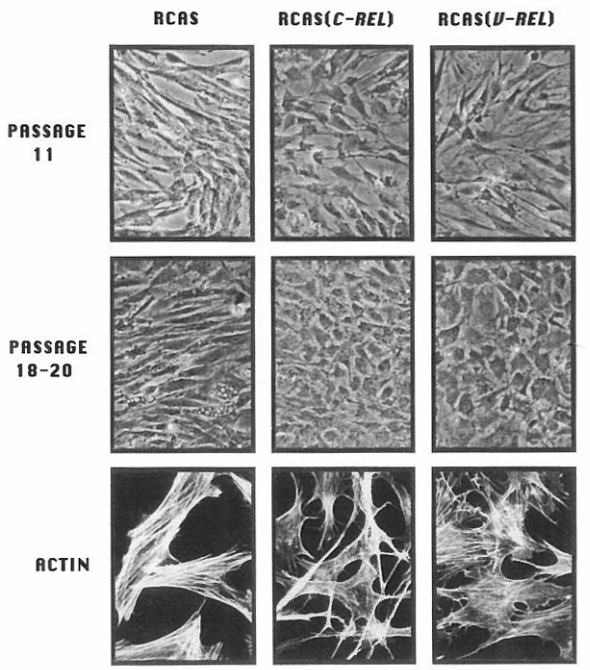

Figure 6. Morphology and Actin Staining of RCAS-Infected, RCAS–c-*rel*–Infected, or RCAS–v-*rel*–Infected CEFs

CEFs transfected with the indicated plasmids (see top of figure) and passaged in culture for various times (indicated at left of figure) were photographed to demonstrate morphology. Alternatively, late passage cells were stained with rhodamine-conjugated phalloidin to stain actin cables (bottom three panels). Note the reduced actin organization in v-*rel*-infected and particularly c-*rel*-infected CEFs as compared with control RCAS-infected CEFs.

p124, active IκB, or both in the cytoplasm. In contrast, RCAS–c-*rel* nuclear extracts gave rise to multiple protein DNA complexes, all of which were recognizable by anti-Rel polyclonal antibody (B_s in Figure 5C, lane 8) and a Rel-reactive monoclonal antibody (data not shown). While these multiple complexes contain Rel-related proteins, their exact composition is unclear at present. The specificity of this interaction was demonstrated by competition with wild-type κB, mutant κB, or a pheromone response element oligonucleotide (data not shown). Thus, nuclear c-Rel from RCAS–c-*rel* CEFs has the ability to bind to a consensus κB site, while the majority of the protein localized in the cytoplasm exhibits little DNA binding.

Biological Effects of Overexpression of c-*rel* in CEF

We next wanted to determine if overexpression of c-*rel* had a detectable effect on normal cell growth, either inducing transformation or cell death as suggested from in situ hybridization studies. v-*rel* induces a transformed phenotype in infected CEFs characterized by alterations in morphology, changes in the organization of actin cables, and an extension of life span in vitro (Franklin et al., 1977; Morrison et al., 1989). Therefore, we examined RCAS–c-*rel*-infected fibroblasts for the expression of these same parameters. As can be seen in Figure 6, RCAS–v-*rel* and RCAS–c-*rel* cells express a characteristic fusiform morphology which becomes more cuboidal on passage, typical of late passage v-*rel*–transformed cells (see progress from early to late passage cells in Figure 6). Interestingly, the onset of the transformed phenotype was delayed in RCAS–c-*rel* cells. Late passage RCAS–c-*rel* CEFs and control RCAS or RCAS–v-*rel* CEFs were next stained with rhodamine-conjugated phalloidin to examine actin cable organization. As can be seen in Figure 6, control late passage RCAS CEFs express well defined actin bundles. In sharp contrast, RCAS–c-*rel* CEFs exhibit extensive actin fiber breakdown, while RCAS–v-*rel* cells lie between these two extremes, showing substantial but not complete disorganization.

Finally, the life span of RCAS–c-*rel*–transformed CEFs was assessed and compared to RCAS–v-*rel* and control RCAS CEFs. RCAS CEFs survived approximately 20–30 passages in culture, at which point, the cells became vacuolated and senesced (note the presence of vacuolated cells in the late passage RCAS CEFs in Figure 6). Both RCAS–v-*rel* and RCAS–c-*rel* fibroblasts, however, continued to grow in culture for more than 60 passages (more than 6 months). Taken together, these experiments suggest that overexpression of c-*rel* induces a phenotype in CEFs similar to v-*rel*. Most notably, like RCAS–v-*rel* CEFs, the life span of RCAS–c-*rel* CEFs is dramatically increased.

Biological Effects of Overexpression of c-*rel* in Avian Bone Marrow Cells

While the pattern of c-*rel* expression during avian embryogenesis suggested a role for c-*rel* in developmental cell death, c-*rel* clearly extended the life span of avian fibroblasts. Because it was possible that c-Rel induced cell death in a cell type–specific way, we examined the consequences of overexpression of c-Rel in another cell type, normal avian hematopoietic cells.

Freshly isolated, total bone marrow cells were cocultivated with RCAS or RCAS–c-*rel* CEFs, as described in Experimental Procedures. After 21 days, no outgrowth was observed in RCAS–c-*rel* bone marrow cultures, while a marginal but reproducible cell outgrowth was observed in normal and RCAS cultures (data not shown). While suggesting that RCAS–c-*rel* was inducing a biological phenotype, these experiments were not conclusive. Therefore, we developed culture conditions that allowed the sustained outgrowth of normal bone marrow cells, which were then infected with RCAS and RCAS–c-*rel* virus and analyzed phenotypically.

Normal bone marrow grown in the presence of transforming growth factor α (TGFα) and stem cell factor (SCF) (Hayman et al., 1993; Williams et al., 1992) could be maintained in culture for periods up to 4 weeks long. Cells, grown under these defined conditions for several days, were then cocultivated with RCAS or RCAS–c-*rel* CEFs in the presence of TGFα and SCF. Two days after cocultivation, RCAS–c-*rel*–infected bone marrow cells began to assume an irregular morphology and settled, while RCAS-infected bone marrow remained in suspension. This morphology became more pronounced with time, and Figure

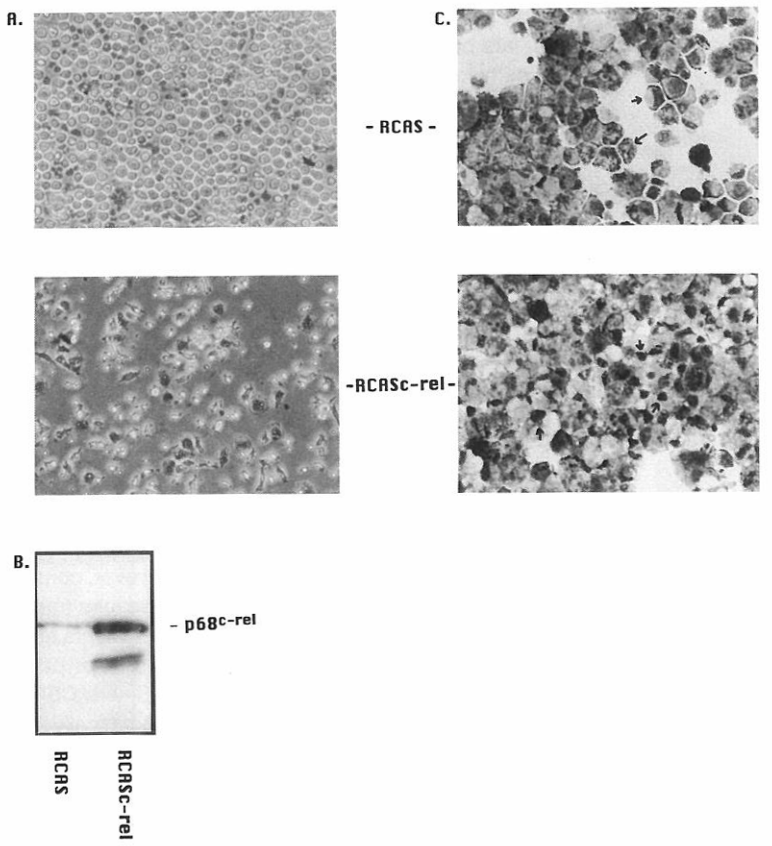

Figure 7. Characterization of RCAS-Infected and RCAS–c-*rel*-Infected Bone Marrow Cells

A) Bone marrow cells from 4- to 10-day old chicks infected with RCAS or RCAS–c-*rel* by cocultivation with infected CEFs were maintained for 6 days in culture, at which time they were photographed. RCAS-infected and RCAS–c-*rel*-infected cultures are indicated. Each was photographed at a magnification of 400×.

(B) Western blot analysis of RCAS-infected and RCAS–c-*rel*-infected bone marrow cells. Equal numbers of bone marrow cells infected as described with RCAS or RCAS–c-*rel* virus were lysed 3–4 days after infection, analyzed by Western blot, and probed with the polyclonal antibody SB66. The c-*rel* protein, $p68^{c\text{-}rel}$, is indicated.

(C) Bone marrow cells (1×10^5) infected as described above were cytospun onto glass slides and stained with Dif-Quick histological stains. RCAS and RCAS–c-*rel* cultures are as indicated. Arrows demonstrate cells containing large nuclei and granules in the RCAS cultures. Condensed darkly staining nuclei are indicated with arrows in the RCAS–c-*rel* culture.

7A shows representative areas within these cultures 6 days after infection.

Given the phenotype observed, it was important to demonstrate that c-Rel was in fact overexpressed in these cells. Equal numbers of RCAS–c-*rel*–infected and RCAS-infected TGFα/SCF cells were harvested 3–4 days after infection and analyzed by Western blot using the polyclonal antibody SB66 that recognized c-Rel. As can be seen in Figure 7B, RCAS–c-*rel* bone marrow cells contain high levels of c-Rel ($p68^{c\text{-}rel}$) when compared to RCAS-infected cells. Proteins at lower molecular weight probably represent proteolytic cleavage products of c-Rel. These results suggest that the phenotype observed in RCAS–c-*rel*-infected TGFα/SCF bone marrow cells is the result of overexpression of c-*rel* in these cells.

To characterize the profound morphological changes induced by c-Rel in more detail, RCAS and RCAS–c-*rel* bone marrow cells were cytospun onto glass slides and stained with the histological dye Dif-Quick (Baxter). As can be seen in Figure 7C, RCAS-infected bone marrow cells are heterogenous, containing blast-like cells with large nuclei, granulated cells reminiscent of promyelocytes, and cells which resemble eosinophils; see arrowed cells in Figure 7C, RCAS (Lucas and Jamroz, 1961). In contrast, RCAS–c-*rel* bone marrow cells are more homogeneous, with very few blast-like cells or granulocytes apparent. Strikingly, in contrast with the RCAS cultures, the majority of the cells contain darkly staining condensed nuclei (see arrowed cells in Figure 7B, RCAS–c-*rel*), a morphology which suggested that RCAS–c-*rel* bone marrow cells were dying, perhaps through programmed cell death or a terminal differentation event. Therefore, we examined the nuclear morphology and growth properties of the cells in greater detail.

RCAS–c-*rel* and RCAS bone marrow cells, infected as described above, were stained using the intercalating DNA dye DAPI. As can be seen in Figure 8A, the nuclei of bone marrow cells infected with the RCAS virus exhibit a relatively uniform distribution of heterochromatin and are generally rounded in shape. Very occasionally, a cell was observed which had either a fragmented or condensed, brightly staining nucleus (data not shown). In contrast, the nuclear staining of RCAS–c-*rel* bone marrow cells was heterogeneous. A large number of the cells had fragmented nuclei, as typified by the arrowed cells in Figure 8A, RCAS–c-*rel* magnified 40×, while the majority of the nuclei had brightly staining margins, suggestive of chromatin margination (Figure 8A, RCAS–c-*rel* magnified 100×). These morphological features are characteristic of cells undergoing the process of programmed cell death (Cohen, 1991; Ellis et al., 1991).

To confirm these observations, an examination of the cells at a more detailed level was required. Therefore, bone marrow cells infected for 6 days with RCAS or RCAS–c-*rel* virus were prepared for examination by electron microscopy (Figure 8B). As can be seen, the nuclei (labeled N) within RCAS-infected bone marrow cells contain large amounts of heterochromatin throughout the nucleus. In

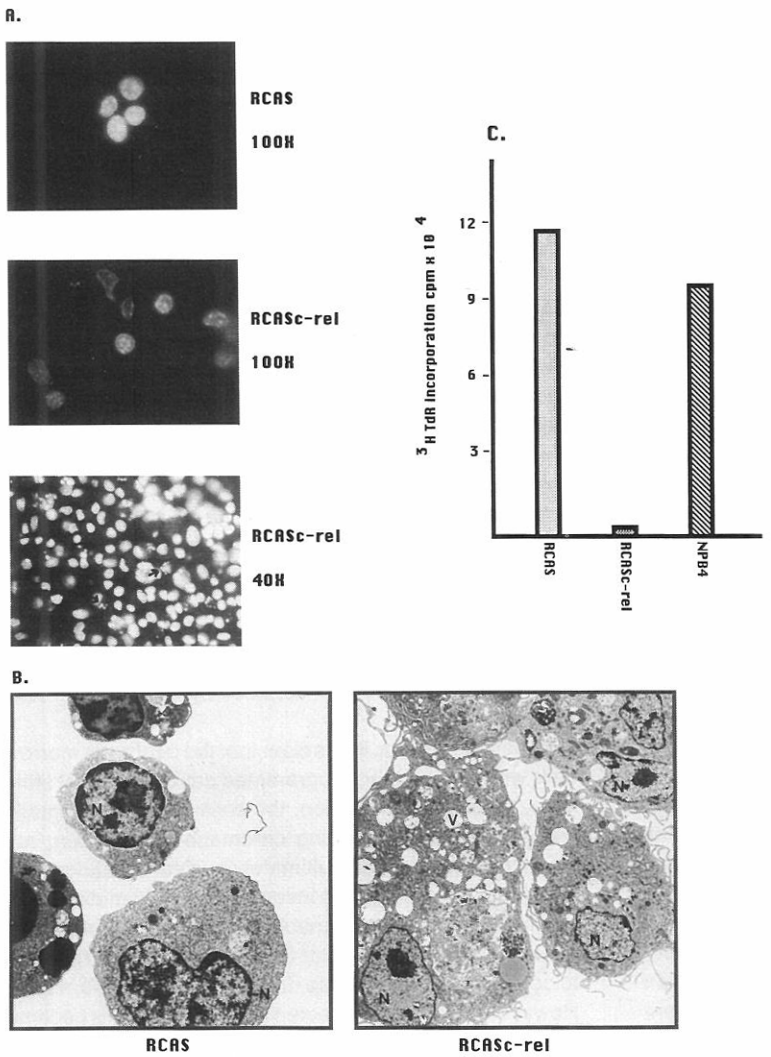

Figure 8. Characterization of Nuclear Morphology and Growth Properties of RCAS and RCAS–c-*rel* Bone Marrow Cells

(A) Bone marrow cells infected as described were harvested 6 days after infection and stained with the intercalating DNA dye DAPI. Examples of RCAS and RCAS–c-*rel* cells photographed at high magnification are shown (RCAS and RCAS–c-*rel*, 100 x). A lower magnification of the RCAS–c-*rel* cells (40 x) is shown to demonstrate the number of cells with the fragmented nuclei in the culture (see arrowed cells).

(B) RCAS-infected or RCAS–c-*rel*-infected bone marrow cells harvested 6 days after infection were prepared for electron microscopy as described in Experimental Procedures. Thin sections were examined at 5,962 x magnification for RCAS and 2,650 x magnification for RCAS–c-*rel* cells. N = nucleus, v = vacuole, I = inclusion body (granule).

(C) RCAS-infected or RCAS–c-*rel*-infected bone marrow cells were harvested 6 days after infection and labeled as described in Experimental Procedures with [^{3}H]thymidine. The level of incorporation of [^{3}H]thymidine was determined as counts per minute (cpm x 10^4). RCAS and RCAS–c-*rel* samples are indicated. As a positive control, v-*rel*-transformed hematopoietic cells, NPB4, were also included (Morrison et al., 1989).

contrast, a ring of condensed chromatin can be observed around the periphery of the nucleus in RCAS–c-*rel* cells. It should also be pointed out that RCAS–c-*rel* cells are much larger than the RCAS cells; however, the organellar organization seems similar. Both RCAS and RCAS–c-*rel* cells have easily identifiable mitochondria and rough endoplasmic reticulum whereas RCAS–c-*rel* cells appear to have more cytoplasmic inclusions and vacuoles (labeled V). RCAS–c-*rel* cells show very little, if any, contraction of the cytoplasm. Thus, the RCAS–c-*rel* bone marrow cells share some but not all of the morphological features attributed to cells undergoing apoptosis. In addition, we have been unable to demonstrate an RCAS–c-*rel*–specific DNA ladder (data not shown). The cytoplasmic changes observed are, in fact, reminiscent of autophagocytosis, which correlates well with our in vivo findings.

These morphological changes suggested that RCAS–c-*rel* bone marrow cells were undergoing programmed cell death. As an extension of our analysis, we carried out a thymidine incorporation assay to confirm that these cells were not replicating their DNA. RCAS or RCAS–c-*rel* bone marrow cells harvested 6 days after infection were pulse labeled with [^{3}H]thymidine (4 μCi/ml) as described and harvested for counting. As can be seen in Figure 8C, RCAS cells incorporated [^{3}H]thymidine as effectively as did the positive control cells, NPB4, a lymphoid cell line transformed by v-*rel* (Morrison et al., 1989). In contrast, very little incorporation was observed with the RCAS–c-*rel* cells, suggesting that overexpression of c-*rel* in bone marrow cells led to cessation of their growth and induced programmed cell death.

Discussion

In this report, we show that c-*rel* is expressed at low levels in most tissues of the chick embryo from E3 to E10. In contrast, high levels are observed in cells undergoing programmed cell death by apoptosis and autophagocytic degeneration. During embryonic development, programmed cell death contributes to sculpturing the body form and provides a means by which unwanted cells can be eliminated without triggering an inflammatory reaction. It is responsible for the destruction of abnormally differentiated cells, like neurons that have made inadequate synaptic

connections, and the elimination of lymphocytes carrying self-reactive receptors (reviewed by Wyllie et al., 1980; Tomei and Cope, 1991). The distinction between apoptosis and autophagocytic cell death is purely morphological and system specific (Clarke, 1990). The first cytologically visible events during apoptosis are chromatin condensation and cytoplasmic compaction. Characteristic fragmentation of the nucleus and cytoplasm into apoptotic bodies follows and may be, but is not necessarily, associated with cleavage of nuclear chromatin into nucleosome-length DNA fragments (Wyllie et al., 1984). Cells undergoing autophagic degeneration exhibit numerous autophagic vacuoles, enlarged organelles, and nuclear pyknosis. While these morphological distinctions are useful in classifying cell death, it is not unusual to find situations that differ from the typical cases just described. For example, apoptosis may occur without characteristic DNA fragmentation (Ellis et al., 1991). Features of both autophagocytic cell death and apoptosis may be found in the same cell, for example within the chick limb bud (Clarke, 1990). Indeed, some cell types, such as chick spinal motor neurons, display great variability in the morphologies of their deaths (Ellis et al., 1991). Thus, differences in the morphology or kinetics of dying cells might reflect distinct mechanisms of cell death or simply differences in the types of cells that are dying. Currently, it is not clear how many distinct mechanisms cause cell death.

Apoptosis occurs as a response to numerous signals, including changes in hormones or cytokine levels or modifications of cell–cell or cell–extracellular matrix interactions. For example, apoptosis in the posterior necrotic zone of the avian limb bud depends on the overlaying ectoderm (Rowe et al., 1982; Hurle and Ganan, 1986; Brewton and MacCabe, 1988), whereas nerve cell death depends on nerve growth factor concentrations (Oppenheim et al., 1988; Batistatou and Greene, 1991). It is not known whether these various stimuli activate different intracellular pathways leading to apoptosis or whether they activate one common pathway. Our in situ hybridization results revealed that c-*rel* is expressed in apoptotic cells in different tissues and in interdigital cells dying by autophagic degeneration. Thus, these studies suggest that c-*rel* might be involved in more than one type of cell death triggered by a variety of signals.

While in situ hybridization data suggested a role for c-*rel* in the process of cell death, it did not establish a functional link. To approach this question, we examined the consequences of c-*rel* overexpression in vitro in two different cell types, avian fibroblasts and bone marrow cells. We ascertained that overexpressed c-Rel in CEFs was regulated normally, since it localized predominantly in the cytoplasm and exhibited DNA binding activity when in the nucleus. Three criteria were used to assess the effects of c-*rel* overexpression in CEFs: morphology, organization of actin cables, and life span. As described, c-*rel* overexpression induced a transformed phenotype in CEF very similar to *v-rel,* albeit with slower kinetics. We do not believe that this delay is due to poor virus spread since the levels of v-*rel* and c-*rel* protein expression were equivalent at the same passage numbers. Perhaps the temporal expression of the transformed phenotype is a reflection of differential regulation of the transcriptional activity of the two proteins. Overexpression of c-*rel* failed to induce apoptosis in CEFs. This is in sharp contrast with overexpressed *c-myc,* which induces cell death in Rat-1 fibroblasts, but only when the cells are grown in low serum. (Evan et al., 1992). Interestingly, RCAS–c-*rel* CEFs grow well at both high and low serum concentrations.

While v-*rel* and c-*rel* appeared to transform CEFs in a similar manner, we were unable to demonstrate any bone marrow–transforming activity associated with c-*rel* expression. In fact, we noted that RCAS–c-*rel*–infected bone marrow cultures routinely failed to grow. On the basis of this observation, we postulated that either RCAS–c-*rel* bone marrow cells required additional growth factors or c-*rel* overexpression prevented the outgrowth of infected cells. To address these questions, we developed culture conditions that allowed normal bone marrow cells to grow for a period of several weeks. When these cells were infected with RCAS or RCAS–c-*rel* virus, RCAS cultures continued to grow and incorporate thymidine. In contrast, RCAS–c-*rel* cultures failed to grow, suggesting that c-*rel* overexpression prevented cell growth, perhaps through a process of programmed cell death or by inducing terminal differentiation.

By several criteria, it was clear that the c-*rel* bone marrow cells were undergoing programmed cell death. Most strikingly, 6 days after infection, the cells exhibited dramatic nuclear changes, including chromatin margination, nuclear condensation, and ultimately nuclear breakdown. In addition, the cells failed to incorporate [^{3}H]thymidine, suggesting that they were unable to replicate DNA. These nuclear changes are similar to those which were reported to occur during the process of apoptosis (Williams, 1991). However, RCAS–c-*rel*–infected bone marrow cells became larger than the normal cells, organellar structures were maintained, and the cells contained numerous vacuoles, reminiscent of autophagocytic cell death (Clarke, 1990) and correlating well with our in vivo results.

Clearly, the biological effects of c-*rel* overexpression in vitro are cell-type specific; while in vivo, dying cells in a wide variety of tissues express high levels of c-*rel*. Taken together, these results suggest that expression of the same gene may lead to physiologically different consequences depending upon the cell type or developmental stage at which it is expressed or the extracellular signals (cytokines, matrix, and cell–cell interactions) received by the cell. Three situations provide support for this notion. Tumor necrosis factor, despite its name, triggers apoptosis in several cell types. In others, it causes activation or differentiation rather than cell death (Laster et al., 1988). While tumor necrosis factor acts at the cell surface to signal these processes, little is known about the downstream effectors which must ultimately be involved in the regulation of gene expression, perhaps genes such as c-*rel*. Secondly, studies on the clonal abortion of autoreactive B cell clones demonstrated that the same signal acting at different developmental stages results in either proliferation and differentiation or cell death (Cohen, 1991; Ellis et al., 1991). If a pre–B cell rearranges its immunoglobulin

genes to produce functional immunoglobulin, it will express surface Immunoglobulin M before Immunoglobulin D. If it sees antigen at this stage, it will be deleted by apoptosis rather than stimulated. If B cell clones survive this stage, however, and see antigen later, they proliferate and differentiate to mature antibody-producing cells. Finally, in the developing avian limb, it was shown that mesenchymal cells of the opaque patch undergo normal cell death in vivo and in organ culture. However, monolayer culture of these cells results in their rescue from cell death. In addition, the cells are prevented from dying by the addition of fibroblast growth factor to organ culture (MacCabe et al., 1991). Thus, the cell type–specific phenotype induced by c-*rel* overexpression in fibroblasts and bone marrow cells may represent the differential response of these cells to the signals that govern proliferation or cell death. This system provides a model in which we can now begin investigating these differences at a biochemical level. For example, the transcription of c-*rel*-regulated genes may be different in the two cell types; perhaps they are governed by alternative protein–protein interactions. Further investigation into the functional properties of c-*rel* and *rel* family members during development will undoubtedly provide greater insight into the role of transcription factors in these key processes. In addition, examination of models such as this will provide further understanding of the mechanism of cell type–specific gene regulation.

Experimental Procedures

cDNA Cloning and Expression

A bursal cDNA library was constructed using the Stratagene ZAP cDNA synthesis kit according to instructions of the manufacturer. The resulting cDNA was packaged using Gigapack 2 Gold packaging extracts (Stratgene) and screened with a v-*rel* (XbaI–NruI) probe. The largest c-*rel* clone (c-*rel* 3B) contained all but 88 bp of 5′ coding sequence. To construct a full-length clone, the 5′ end of c-*rel* derived from a HP46 cell line cDNA library (Kabrun et al., 1990) was ligated to the c-*rel*3B clone at the unique ScaI site. These sequences are identical to previously published sequences (Capobianco et al., 1990) except that they encode an isoleucine (Ile) to leucine (Leu) change at amino acid 205, a Glutamine (Gln), Leu to histidine (His), Valine (Val) change at amino acids 367 and 368, and a glycine (Gly) to serine (Ser) change at amino acid 410. To express the c-*rel* cDNA in avian cells, pBSc-*rel* was digested with KspI and NaeI to release the coding sequences of c-*rel*, which were blunt ended using standard protocols (Ausubel et al., 1987) and ligated into pRCAS, a replication-competent retroviral vector (Hughes et al., 1987).

Synthesis of [^{35}S]RNA Probes

The chicken full-length c-*rel* cDNA was cloned into the expression vector Bluescript SK− (Stratagene) which has both T3 and T7 RNA polymerase promoters. Because c-Rel protein is 70% homologous in the amino terminal region to the two components of the NF-κB transcription factor complex (Ghosh et al., 1990; Nolan et al., 1991), probes specific for c-*rel* were required to ensure the specificity of hybridization. Therefore, the full-length cDNA was digested by BamHI, which removes the 5′ 1 kb fragment containing the conserved part of the molecule. The remaining c-*rel*-specific 3′ 2.8 kb fragment was subcloned into the Bluescript expression vector. [^{35}S]RNA probes were transcribed from 2 μg of linearized plasmids by 20 U of either T7 RNA polymerase for antisense probes or T3 RNA polymerase for sense probes in a 20 μl reaction mixture containing 200 μCi [^{35}S]CTP (1300 Ci/mmol), 20 mM UTP, ATP, and GTP for 2 hr at 39°C. To facilitate their penetration into cells, probes were submitted to a limited alkaline hydrolysis, generating fragments of approximately 150 bases as recommended by Cox et al. (1984).

Embryonic Tissue Preparation and In Situ Hybridization

Brown leghorn chicken eggs were incubated at 37°C in a humidified chamber. The age of embryos is indicated as E1, E2, etc. (E1 corresponding to 24 hr of incubation, E2 to 48 hr, etc.). Whole embryos or dissected tissues were fixed at 4°C for 18 hr in 4% paraformaldehyde in phosphate-buffered saline (PBS) (Na_2HPO_4–$NaHPO_4$ 0.1 M [pH 7.4]), embedded in paraffin, and processed for histological sections.

In situ hybridization was adapted from the method of Cox et al. (1984), as described by Quéva et al. (1992). Briefly, after being deparaffinized and rehydrated, sections were incubated in 0.1 M Gly, 0.2 M Tris–HCl (pH 7.4) for 10 min at 20°C, treated with 1 μg/ml proteinase K (Boehringer Mannheim) for 15 min at 37°C, post-fixed in 4% paraformaldehyde, washed in PBS, acetylated for 10 min with 0.25% acetic anhydride in 0.1M triethanolamine, washed in 2× SSC (20× SSC = 3M NaCl, 0.3M sodium citrate), and dehydrated by ethanol.

[^{35}S]RNA probes were denatured at 80°C and diluted in the hybridization buffer (Cox et al., 1984) at a concentration of 50 pg/μl. Hybridization was performed at 60°C for 18 hr. After a wash in 4× SSC at 20°C, slides were treated with 10 μg/ml of RNAase A (type III A, Sigma) for 30 min at 37°C, subsequently washed in 0.1 × SSC at 60°C, dehydrated by ethanol, and dipped in nuclear track emulsion (Kodak NTB2). The slides were exposed at 4°C for 2–4 weeks. After developing, slides were stained with a DNA intercalating fluorescent dye (Hoechst 33258), mounted, and observed under dark-field and ultraviolet illumination with a Zeiss microscope.

Cell Culture

CEFs were grown in Dulbecco's modified Eagle's medium supplemented with 10% heat-inactivated fetal calf serum, 2% heat-inactivated chicken serum, 100 U of penicillin/ml, 100 μg streptomycin/ml, 1 mM sodium pyruvate, 0.1 mM nonessential amino acids and, additionally, 2 mM L-glutamine (all tissue culture media were purchased from GIBCO Laboratories) at 37°C. CEFs were prepared and cultured as described previously (Morrison et al., 1989). Transfection of CEFs with RCAS or RCAS–c-*rel* plasmid DNA was carried out following the procedures of Chen and Okayama (1987). Bone marrow cells were isolated from 4- to 10-day old chicks as described previously (Boehmelt et al., 1992; Morrison et al., 1989). Subsequently, they were grown for 4 days in S13 Dulbecco's modified Eagle's medium (Larsen et al., 1992) and supplemented with TGFα (Promega) at a concentration of 5 ng/ml and avian SCF (provided by Dr. F. Martin, Amgen) at a concentration of 50 ng/ml. Cells were fed daily with fresh medium and growth factor.

Infection of bone marrow was carried out by cocultivation with RCAS or RCAS–c-*rel* virus-producing CEFs. After 2 days of cocultivation, bone marrow cells were removed from the fibroblast monolayer and propagated in S13 Dulbecco's modified Eagle's medium, supplemented as described above, with TGFα and SCF. Infected bone marrow cells (1×10^5 cells) were cytospun onto glass slides 6 days after infection and stained using Dif-Quick (Baxter). They were then photographed using Kodak 160-T film.

Immunofluorescence

Cells, fixed by the addition of 3% formaldehyde in PBS (0.15M NaCl, 0.1M Na_2HPO_4, 0.1M NaH_2PO_4), were stained with the affinity purified primary rabbit antibody SB66 at a dilution of 1/50 followed by secondary fluorescein isothiocyanate–conjugated goat anti-rabbit antibody (ICN Biomedical), as described previously (Morrison et al., 1989). To stain for actin cables, cells were stained with rhodamine-conjugated phalloidin according to the instructions of the manufacturer (Molecular Probes).

Cell Fractionation and Western Blotting

Cell fractionation was carried out following the protocols described in Morrison et al., (1989). Whole cells or nuclear and cytoplasmic fractions were subjected to Western blot analysis (Towbin et al., 1979) and probed with a polyclonal antibody SB66 that recognizes both v-*rel* and c-*rel* (Kabrun et al., 1991; Morrison et al., 1989). Detection of protein antibody complexes was carried out using the Enhanced Chemiluminescence system (ECL, Amersham). Alternatively, total embryos or individual organs at various developmental stages were dissected in PBS, transferred to a solution containing 0.06 M Tris–HCl (pH 6.8), 5% β-mercaptoethanol, 2% SDS–polyacrylamide gel, 10% glycerol, 0.002% bromophenol blue, and suspended by dounce ho-

mogenization; samples were then sonicated, centrifuged at 10,000 × g, and equal amounts of protein were subjected to Western blot analysis (Towbin et al., 1979). Nitrocellulose filters were probed with a 1:2000 dilution of purified serum SB 146 specifically directed against the carboxy terminal 15 amino acids of chicken *c-Rel* protein (P. E., unpublished data). Detection of protein–antibody complexes was accomplished using horseradish peroxidase–conjugated swine anti-rabbit immunoglobulin (1:500, Dakopatts) and incubation in diaminobenzidine (30 mg in 100 ml 0.05 M Tris–HCl [pH 7.4], 0.01% H_2O_2).

Electrophoretic Mobility Shift Assays

Electrophoretic mobility shift assays were performed essentially as described previously (Kabrun et al., 1991), using nuclear or S100 extracts from transfected CEFs, prepared as described by Dignam et al. (1983). Incubation buffer contained 0.5 μg salmon sperm DNA, 10 mM Tris–HCl (pH 7.5), 5 mM NaCl, 1 mM dithiothreitol, 1 mM EDTA, 5% glycerol, and 3 mM dGTP. Oligonucleotide sequences are as published previously (Kabrun et al., 1991).

DAPI Staining

Bone marrow cells (1×10^5) infected for 6 days with RCAS or RCAS–c-*rel* virus were stained using the intercalating DNA dye DAPI (Boerhinger Mannheim), following the manufacturer's protocol. After staining, the cells were mounted on glass slides in Mowiol (Hoescht) and photographed.

Electron Microscopy

Bone marrow cells (1×10^6) infected for 6 days with RCAS or RCAS–c-*rel* virus were fixed in 3% glutaraldehyde in PBS overnight and processed for electron microscopy following the procedures outlined in Hayat (1974).

[^{3}H]Thymidine Uptake

Bone marrow cells (2×10^4) infected for 6 days with RCAS or RCAS–c-*rel* virus were suspended in 50 μl of S13 Dulbecco's modified Eagle's medium, incubated with [^{3}H]thymidine (4 μCi/ml, Amersham) for 2 hr, and harvested onto glass fiber filters as described (Leutz et al., 1984).

Characterization of DNA Degradation

Embryos, dissected in PBS, were Dounce homogenized in STE (Tris–HCl 10 mM [pH 7.5], NaCl 10 mM, EDTA 10 mM). High molecular weight DNA was prepared following standard protocols (Ausubel et al., 1987). Total DNA (1 μg) was labeled with ^{32}P using Klenow polymerase according to Rösl (1992). Samples were electrophoresed on 1.8% agarose gels and the DNA visualized by autoradiography. As a positive control, we used DNA from dexamethasone-treated S49.1 mouse thymocytes (Ucker, 1987).

Acknowledgments

C. A. and N. K. share equal status as coauthors for this paper. We are grateful to Marie Anne Mirabel for her work in the first series of experiments with the c-*rel* probe and Anne Verdeil for her help in the characterization of the DNA ladders. We are indebted to Christophe Quéva for his help in designing the in situ hybridization protocol as well as for providing invaluable advice on the technique. We also thank Xavier Desbiens, Jean Claude Ameisen, Veronique Fafeur, and members of the Enrietto lab for critical reading of this manuscript and Nicole Devassine for patient typing. We are particularly indebted to Susanne Meyer for technical support and Alan Jones for electron microscopy. This work was supported by grants from the National Insititutes of Health (NIH) CA51792 and the Council for Tobacco Research #3196, the Institut Pasteur de Lille, the Centre National de la Recherche Scientifique, the Association pour la Recherche sur le Cancer, and the Ligue Nationale contre le Cancer. N. K. was supported by a training grant from NIH to the Department of Microbiology of the State University of New York at Stony Brook (NIH 5T32CA09176). This work is dedicated to the memory of Dr. Donna S. Coffman.

Received June 18, 1993; revised September 6, 1993.

References

Ausubel, F. M., Brent, R., Kingston, R. E., Moore, D. D., Seidman, J. G., Smith, J. A., and Struhl, K. (1987). Current Protocols in Molecular Biology (New York: Wiley-Interscience).

Baeuerle, P. A. (1991). The inducible transcription activator NF-κB: regulation by distinct protein subunits. Biochim. Biophys. Acta. *1072*, 63–80.

Ballard, D. W., Dixon, E. P., Peffer, N. J., Bogerd, H., Doerre, S., Stein, B., and Green, W. C. (1992). The 65-kDa subunit of human NF-κB functions as a potent transcriptional activator and a target for v-Rel-mediated repression. Proc. Natl. Acad. Sci. USA *89*, 1875–1879.

Barth, C. F., and Humphries, E. H. (1988). A non-immunosuppressive helper virus allows high efficiency induction of B-cell lymphomas by reticuloendotheliosis virus strain T. J. Exp. Med. *167*, 89–108.

Batistatou, A., and Greene, L. A. (1991). Aurintricarboxylic acid rescues PC12 cells and sympathetic neurons from cell death caused by nerve growth factor deprivation: correlation with suppression of endonuclease activity. J. Cell Biol. *115*, 461–471.

Beug, H., Muller, H., Doederlein, G., and Graf, T. (1981). Hematopoietic cells transformed *in vitro* by REV-T avian reticuloendotheliosis virus express characteristics of very immature lymphoid cells. Virology *115*, 295–309.

Boehmelt, G., Walker, A., Kabrun, N., Mellitzer, G., Beug, H., Zenke, M., and Enrietto, P. J. (1992). Hormone-regulated v-*rel* estrogen receptor fusion protein: reversible induction of cell transformation and cellular gene expression. EMBO J. *11*, 4641–4652.

Brewton, R. G., and MacCabe, J. A. (1988). Ectodermal influence on physiological cell death in the posterior necrotic zone of the chick wing bud. Dev. Biol. *16*, 327–330.

Brownell, E., Mathieson, B., Young, H. A., Keller, J., Ihle, J. N., and Rice, N. R. (1987). Detection of c-*rel*-related transcripts in mouse hematopoietic tissues, fractionated lymphocyte populations and cell lines. Mol. Cell. Biol. *7*, 1304–1309.

Capobianco, A. J., and Gilmore, T. D. (1991). Repression of the chicken c-*rel* promoter by v-*rel* in chicken embryo fibroblasts is not mediated through a consensus NF-κB binding site. Oncogene *6*, 2203–2210.

Capobianco, A. J., Chang, D., Mosialos, G., and Gilmore, T. D. (1992). p105, the NF-κB p50 precursor protein, is one of the cellular proteins complexed with the v-Rel oncoprotein in transformed chicken spleen cells. J. Virol. *66*, 3758–3767.

Capobianco, A. J., Simmon, D. L., and Gilmore, T. D. (1990). Cloning and expression of a chicken c-rel cDNA: unlike $p59^{v\text{-}rel}$, $p68_{c\text{-}rel}$ is a cytoplasmic protein in chicken embryo fibroblasts. Oncogene *5*, 257–265.

Chen, C., and Okayama, H. (1987). High efficiency transformation of mammalian cells by plasmid DNA. Mol. Cell. Biol. *7*, 2745–2752

Clarke, P. G. H. (1990). Developmental cell death: morphological diversity and multiple mechanisms. Anat. Embryol. *181*, 195–213.

Cohen, J. J. (1991). Programmed cell death in the immune system. Adv. Immunol. *50*, 55–85.

Cox, K. H., DeLeon, D. V., Angerer, L. M., and Angerer, R. C. (1984). Detection of mRNAs in sea urchin embryos by *in situ* hybridization using asymmetric RNA probes. Dev. Biol. *101*, 485–502.

Davis, J. N., Bargmann, W., and Bose, Jr., H. R. (1990). Identification of protein complexes containing the c-*rel* protooncogene product in avian hematopoietic cells. Oncogene *5*, 1109–1115.

Davis, N., Ghosh, S., Simmons, D. L., Tempst, P., Liou, H., Baltimore, D., and Bose, Jr., H. R. (1991). Rel-associated pp40: an inhibitor of the *rel* family of transcription factors. Science *253*, 1268–1271.

Dignam, J. P., Lebovitz, R. M., and Roeder, R. G. (1983). Accurate transcription initiation by RNA polymerase II in a soluble extract from isolated mammalian nuclei. Nucl. Acids Res. *11*, 1475–1489.

Ellis, R. E., Yuan, J., and Horvitz, H. R. (1991). Mechanisms and functions of cell death. Annu. Rev. Cell Biol. *7*, 663–698.

Evan, G. I., Wyllie, A. H., Gilbert, C. S., Littlewood, T. D., Land, H., Brooks, M., Waters, C. M., Penn, L. Z., and Hancock, D. C. (1992). Induction of apoptosis in fibroblasts by c-myc protein. Cell *69*, 119–128.

Franklin, R. B., Kang, C. Y., Wan, M. K., and Bose, Jr., H. R. (1977).

Transformation of chick embryo fibroblasts by reticuloendotheliosis virus. Virology *83*, 313–321.

Fujita, T., Nolan, G. P., Ghosh, S., and Baltimore, D. (1992). Independent modes of transcriptional activation by the p50 and p65 subunits of NF-κB. Genes Dev. *6*, 775–787.

Ghosh, S., Gifford, A. M., Riviere, L. R., Tempst, P., Nolan, G. P., and Baltimore, D. (1990). Cloning of the p50 DNA binding subunit of NF-κB: homology to *rel* and *dorsal*. Cell *62*, 1019–29.

Gilmore, T. D., and Temin, H. M. (1986). Different localization of the product of the v-*rel* oncogene in chicken fibroblasts and spleen cells correlates with transformation by REV-T. Cell *44*, 791–800.

Grumont, R. J., and Gerondakis, S. (1990a). The murine c-*rel* proto-oncogene encodes two mRNAs the expression of which is modulated by lymphoid stimuli. Oncogene Res. *5*, 245–254.

Grumont, R. J., and Gerondakis, S. (1990b). Murine c-*rel* transcription is rapidly induced in T-cells and fibroblasts by mitogenic agents and the phorbol ester 12-O-tetradecanoylphorbol-13-acetate. Cell Growth Differ. *1*, 345–350.

Hannink, M., and Temin, H. M. (1990). Structure and autoregulation of the c-*rel* promoter. Oncogene *5*, 1843–1850.

Hansen, S. K., Nerlov, C., Zabel, U., Verde, P., Johnsen, M., Baeuerle, P. A., and Blasi, F. (1992). A novel complex between the p65 subunit of NF-κB and c-*rel* binds to a DNA element involved in the phorbol ester induction of the human urokinase gene. EMBO J. *11*, 205–213.

Hayat, M. A. (1973). Electron Microscopy of Enzymes, Volume 1 (New York: van Nostrand and Rienhold).

Hayat, M. A. (1974). Electron Microscopy of Enzymes, Volume 2 (New York: van Nostrand and Reinhold).

Hayman, M. J., Meyer, S., Martin, F., Steinlein, P., and Beug, H. (1993). Self-renewal and differentiation of normal avian erythroid progenitor cells: regulatory roles of the TGFα/c-ErbB and SCF/c-Kit receptors. Cell *74*, 157–169.

Hinchliffe, J. R., and Ede, D. A. (1973). Cell death and the development of limb form and skeletal pattern in normal and *wingless* (ws) chick embryos. J. Embryol. Exp. Morphol. *30*, 753–772.

Hughes, S. H., Greenhouse, J. J., Petropouls, C. J., and Sutrave, P. (1987). Adaptor plasmids simplify the insertion of foreign DNA into helper-independent retroviral vectors. J. Virol. *61*, 3004–3012.

Hurle, J. M., and Ganan, Y. (1986). Interdigital tissue chondrogenesis induced by surgical removal of the ectoderm in the embryonic chick leg bud. J. Embryol. Exp. Morphol. *94*, 231–244.

Inoue, J., Kerr, L. D., Ransone, L. J., Bengal, E., Hunter, T., and Verma, I. M. (1991). c-*rel* activates but v-*rel* suppresses transcription from κB sites. Proc. Natl. Acad. Sci. USA *88*, 3715–3719.

Inoue, J., Kerr, L. D., Rashid, D., Davis, N., Bose, Jr., H. R., and Verma, I. M. (1992). Direct association of pp40/IκBβ with rel/NF-κB transcription factors: role of ankyrin repeats in the inhibition of DNA binding activity. Proc. Natl. Acad. Sci. USA *89*, 4333–4337.

Kabrun, N., Bumstead, N., Hayman, M. J., and Enrietto, P. J. (1990). Characterization of a novel promoter insertion in the c-*rel* locus. Mol. Cell. Biol. *10*, 4788–4794.

Kabrun, N., Hodgson, J. W., Doemer, M., Mak, G., Franza, B. R., and Enrietto, P. J. (1991). Interaction of the v-*rel* protein with an NF-κB DNA binding site. Proc. Natl. Acad. Sci. USA *88*, 1783–1787.

Kerr, L. D., Inoue, J., Davis, N., Link, E., Baeuerle, P. A., Bose Jr., H. R., and Verma, I. M. (1991). The rel-associated pp40 protein prevents DNA binding of Rel and NF-κB: relationship with IκBb and regulation by phosphorylation. Genes Dev. *5*, 1464–1476.

Kieran, M., Blank, V., Logeat, F., Vandekerckhove, J., Lottspeich, F., Le Bail, O., Urban, M. B., Kourilsky, P., Baeuerle, P. A., and Israël, A. (1990). The DNA binding subunit of NF-κB is identical to factor KBF1 and homologous to the *rel* oncogene product. Cell *62*, 1007–1018.

Kochel, T., and Rice, N. R. (1992). v-*rel* and c-*rel*-protein complexes bind to the NF-κB site *in vitro*. Oncogene *7*, 567–572.

Kochel, T., Mushinski, J. F., and Rice, N. R. (1991). The v-*rel* and c-*rel* proteins exist in high molecular weight complexes in avian and murine cells. Oncogene *6*, 615–626.

Larsen, J., Beug, H., and Hayman, M. J. (1992). The *v-ski* oncogene cooperates with the *v-sea* oncogene in erythroid transfortmation by blocking erythroid differentiation. Oncogene *7*, 1903–1911.

Laster, S. M., Wood, J. G., and Gooding, L. R. (1988). Tumor Necrosis Factor can induce both apoptotic and necrotic forms of cell lysis. J. Immunol. *141*, 2629–2634.

Leutz, A., Beug, H., and Graf, T. (1984). Purification and characterization of cMGF, a novel chicken myelomonocytic growth factor. EMBO J. *3*, 3191–3197.

Lewis, R. B., McClure, J., Rup, B., Niesel, D. W., Garry, R. F., Hoelzer, J. D., Nazerian, K., and Bose, Jr., H. R. (1981). Avian reticuloendotheliosis virus: identification of the hematopoietic target cell for transformation. Cell *25*, 421–431.

Lucas, A. M., and Jamroz, L.(1961). Atlas of Avian Hematology: Agricultural Monograph 25 (Washington, DC: United States Department of Agriculture).

MacCabe, J. A., Blaylock, R. L., Latimer, J. L., and Pharris, L. J. (1991). Fibroblast growth factor and culture in monolayer rescue mesoderm cells destined to die in the developing avian wing. J. Exp. Zool. *257* 208–213.

Moore, B. E., and Bose, Jr., H. R. (1989). Expression of the c-*rel* and *c-myc* proto-oncogenes in avian tissues. Oncogene *4*, 845–852.

Morrison, L. E., Boehmelt, G., and Enrietto, P. J. (1992). Mutations in the *rel*-homology domain alter the biochemical properties of v-rel and render it transformation defective in chicken embryo fibroblasts. Oncogene *7*, 1137–1147.

Morrison, L. E., Boehmelt, G., Beug, H., and Enrietto, P. J. (1991). Expression of v-*rel* by a replication-competent virus: transformation and biochemical characterization. Oncogene *6*, 1657.

Morrison, L. E., Kabrun, N., Mudri, S., Hayman, M. J., and Enrietto, P. J. (1989). Viral *rel* and cellular *rel* associate with cellular proteins in transformed and normal cells. Oncogene *4*, 677–683.

Nakayama, K., Shimizu, H., Mitomo, K., Watanabe, T., Okamoto, S.-I., and Yamamoto, K.-I. (1992). A lymphoid cell-specific nuclear factor containing c-Rel-like proteins preferentially interacts with interleukin-6 κB-related motifs whose activities are repressed in lymphoid cells. Mol. Cell. Biol. *12*, 1736–1746.

Neiman, P. E., Thomas, S. J., and Loring, G. (1991). Induction of apoptosis during normal and neoplastic B-cell development in the bursa of Fabricius. Proc. Natl. Acad. Sci. USA *88*, 5857–5861.

Neri, A., Chang, C.-C., Lombardi, L., Salina, M., Corradini, P., Maiolo, A. T., Chaganti, R. S. K., and Dalla-Favera, R. (1991). B cell lymphoma-associated chromosomal translocation involves candidate oncogene *lyt-10*, homologous to NF-κB p50. Cell *67*, 1075–1087.

Nolan, G. P., and Baltimore, D. (1992). The inhibitory ankyrin and activator Rel proteins. Curr. Opin. Genet. Dev. *2*, 211–220.

Nolan, G. P., Ghosh, S., Liou, H.-C., Tempst, P., and Baltimore, D. (1991). DNA binding and IκB inhibition of the cloned p65 subunit of NF-κB, a *rel*-related polypeptide. Cell *64*, 961–969.

Oppenheim, R. W., Haverkamp, L. J., Prevette, D., McManaman, J. L., and Apel, S. H. (1988). Reduction of naturally occurring motorneuron death *in vivo* by a target-derived neurotrophic factor. Science *240*, 919–922.

Perkins, N. D., Schmid, R. M., Duckett, C. S., Leung, K., Rice, N. R., and Nabel, G. J. (1992). Distinct combinations of NF-κB subunits determine the specificity of transcriptional activation. Proc. Natl. Acad. Sci. USA *89*, 1529–1533.

Quéva, C., Ness, S. A., Graf, T., Vandenbunder, B., and Stéhelin, D. (1992). Expression patterns of *c-myb* and of *v-myb* induced myeloid-1 (*mim-1*) gene during the development of the chick embryo. Development *114*, 125–133.

Reddy, E., Skalka, A., and Curran, T. (1988). The Oncogene Handbook (Amsterdam: Elsevier).

Rice, N. R., MacKichan, M. L., and Israël, A. (1992). The precursor of NF-κB p50 has IκB-like functions. Cell *71*, 243–253.

Rösl, F. (1992). A simple and rapid method for detection of apoptosis in human cells. Nucl. Acids Res. *20*, 5243.

Rowe, D. A., Cairns, J. M., and Fallon, J. F. (1982). Spatial and tempo-

ral patterns of cell death in limb bud mesoderm after apical ectodermal ridge removal. Dev. Biol. *93*, 83–91.

Ryseck, R. P., Bull, P., Takamiya, M., Bours, V., Siebenlist, U., Dobrzanski, P., and Bravo, R. (1992). RelB, a new Rel family transcription activator that can interact with p50-NF-κB. Mol. Cell. Biol. *12*, 674–684.

Simek, S., and Rice, N. R. (1988). Detection and characterization of the protein encoded by the chicken c-*rel* protooncogene. Oncogene Res. *2*, 103–119.

Steward, R., Ambrosio, L., and Schedl, P. (1985). Expression of the *dorsal* gene. Cold Spring Harbor Symp. Quant. Biol. *50*, 223–228.

Tan, T. H., Huang, G. P., Sica, A., Ghosh, P., Young, H. A., Longo, D. L., and Rice, N. R. (1992). κB site-dependent activation of the interleukin-2 receptor alpha-chain gene promoter by human c-*rel*. Mol. Cell. Biol. *12*, 4067–4075.

Tomei, L. D., and Cope, F. O. (1991). Apoptosis: The Molecular Basis of Cell Death (Cold Spring Harbor, New York: Cold Spring Harbor Laboratory Press).

Towbin, H., Staehelin, T., and Gordon, J. (1979). Electrophoretic transfer of proteins from polyacrylamide gels to nitrocellulose sheets: procedure and some applications. Proc. Natl. Acad. Sci. USA *76*, 4350–4354.

Ucker, D. S. (1987). Cytotoxic T lymphocytes and glucocorticoids activate an endogenous suicide process in target cells. Nature *327*, 62–64.

Williams, G. T. (1991). Programmed cell death: apoptosis and Oncogenesis. Cell *65*, 1097–1098.

Williams, D. E., de Vries, Peter, Namen, A. E., Widmer, M. B., and Lyman, S. (1992), The steel factor. Dev. Biol. *151*, 368–376.

Wyllie, A. H., Kerr, J. F. R., and Currie, A. R. (1980). Cell death: the significance of apoptosis. Int. Rev. Cytol. *68*, 251–306.

Wyllie, A. H., Morris, R. G., Smoth, A. L., and Dunlop, D. (1984). Chromatin cleavage in apoptosis: association with condensed chromatin morphology and dependence on macromolecular synthesis. J. Pathol. *142*, 67–77.